Nonstationary phase shift (NSPS) for TI media

Robert J. Ferguson and Gary F. Margrave

ABSTRACT

Nonstationary phase shift (NSPS) can be modified, using vertical and horizontal slowness, to extrapolate wavefields through media that are transversely isotropic (TI), and whose elastic parameters vary laterally. No restriction is placed on the weakness of the anisotropy, or the angle of TI symmetry. The significance of this method lies in the fact that velocity variation is allowed simultaneously in space and spatial frequency, and that wavefield extrapolation proceeds using only phase velocity.

We present impulse responses for P-waves for a number of different TI media. The first, weathered gypsum, was chosen due to its extreme P-wave anisotropy (82%). The second, Mesaverde shale, was chosen due to its more typical anisotropy (13%). Impulse responses are computed for the isotropic, vertical TI and TI with different axes of symmetry (-45 degrees for weathered gypsum, 60 degrees for Mesaverde shale). The responses for the weathered gypsum show significant anisotropic effects, particularly for dipping angle of symmetry. The Mesaverde shale responses are less significant due to the lower level of anisotropy.

To demonstrate NSPS for materials with lateral variation in anisotropy, we present a scenario where two spatially separate impulses are extrapolated simultaneously through a 300-meters of Gypsum and Mesaverde shale. The weathered Gypsum grades abruptly into Mesaverde shale, both having different axis of YI symetry. The resulting responses match those from the constant anisotropy cases.

INTRODUCTION

The notion that seismic anisotropy is intrinsic to wavefield propagation in the subsurface is swiftly gaining recognition as a factor in imaging. Though anisotropy is reported throughout the earth's' crust and upper mantle (Crampin, 1984) the special case of transverse isotropy (TI) is sufficiently common to warrant consideration (Byun, 1984). One of the most mathematically tractable forms of anisotropy, TI describes a medium in which a large number of homogeneous, isotropic layers are arranged in alternating planes, such that five elastic parameters provide a complete description of the mediums' elastic properties (see, for example, Postma, 1955). In such a medium, for wavelengths much longer than the layer thicknesses, we find that all directions relative to the same axis of symmetry are equivalent (again, Postma, 1955).

Thomsen (1986) points out the fundamental inconsistency of trying to image a potentially anisotropic subsurface using the assumption of isotropy. Isaac and Lawton (1997) demonstrate the peril of imaging TI media with standard isotropic processing. In a physical modeling experiment they show that that a medium with ~20% P-wave anisotropy and a TI symmetry of 45 degrees causes large errors in the lateral position of a simulated reef edge.

Authors such as Uzcategui (1995), Kitchenside (1993), and Kitchenside (1991) have proposed algorithms by which TI media might be imaged. However, their algorithms are based on ω -x extrapolation techniques which Margrave and Ferguson (1997) and Black et al. (1984) point out are space domain approximations to a nonstationary Fourier operator. Authors such as Margrave and Ferguson (1997), Black et al. (1984) and Wapenaar (1994) show that a wavefield extrapolation scheme can be formulated in Fourier space, that is $(\omega - k_x)$, which requires no approximation to cope with laterally varying velocities. Margrave and Ferguson (1997) refer to this scheme as NSPS (nonstationary phase shift).

In this paper we present an extension of NSPS to handle TI media. This, we will show, is done without approximation of the extrapolator, without restriction of the TI axis of symmetry, and without restricting the weakness/strongness of the anisotropy. We will use Thomsen parameters to describe the anisotropy.

Examples of impulse responses are presented to demonstrate the ability of TI NSPS to handle laterally variant anisotropic parameters.

NONSTATIONARY PHASE SHIFT

Wavefield extrapolation by nonstationary phase shift is an extrapolation method suitable for depth migration or modeling. It proposes that, based on the scalar wave equation, the Fourier domain $(\omega - k_x)$ provides a complete description of the subsurface which can be developed using the theory of nonstationary filters. (For a detailed description of NSPS we refer the reader to Margrave and Ferguson,1997.)

Though Margraves' filter theory (1997) provides prescriptions for space $(\omega - x)$ (ω -x) and dual $(\omega - (x, k_x))$ as well as the Fourier domain, we presently prefer to use the Fourier domain description. This is due mainly to the fact that there are significant runtime advantages to using this domain (Ferguson and Margrave, 1997, Margrave and Ferguson, 1997, and Wapenaar, 1994).

The basic equation for Fourier domain NSPS is:

$$\varphi(k_x, \Delta z, \omega) = \int_{-\infty}^{\infty} \varphi(k'_x, 0, \omega) A(k_x, k_x - k'_x, \omega) dk'_x \qquad (1)$$

where, $\varphi(k_x, \Delta z, \omega)$ is the Fourier transform of the wavefield (output) which has been extrapolated one depth step (Δz) from a reference depth $z = 0$; $\varphi(k'_x, \Delta z, \omega)$ is the Fourier transform of the wavefield (input) recorded at the reference depth $z = 0$ (the primes in equation (1) are used to distinguish input from output wavenumbers - see Margrave and Ferguson, 1997). The operator $A(k_x, k - k'_x, \omega)$ is essentially a shifted Fourier transform of the nonstationary wavefield extrapolator and is computed as:

$$A(k_x, k_x - k_x', \omega) = \int_{-\infty}^{\infty} \alpha(k_x, x', \omega) e^{-ix'(k_x - k_x')} dx' \tag{2}$$

where,

$$\alpha(k_x, x', \omega) = \left\{ \begin{matrix} e^{ik_z(k_x, x', \omega)\Delta z}, \frac{\omega^2}{v^2(x')} - k_x^2 \geq 0 \\ e^{i|\mathrm{Im}(k_z(k_x, x', \omega))|\Delta z}, \frac{\omega^2}{v^2(x')} - k_x^2 < 0 \end{matrix} \right\}, k_z(k_x, x', \omega) = \sqrt{\frac{\omega^2}{v^2(x')} - k_x^2} \tag{3}$$

is the nonstationary extrapolator (Margrave and Ferguson, 1997).

Equation (3) insures exponential decay of energy in the evanescent region (k_x is imaginary). The operator in equation (3) is an isotropic function of laterally variable velocity. We propose that $v(x')$ be extended to vary with angle of incidence thus, $v(x') \rightarrow v(k_x, x')$, and Equation (3) becomes the TI nonstationary extrapolator:

$$\alpha(k_x, x', \omega) = \left\{ \begin{matrix} e^{ik_z(k_x, x', \omega)\Delta z}, \frac{\omega^2}{v^2(x', k_x)} - k_x^2 \geq 0 \\ e^{i|\mathrm{Im}(k_z(k_x, x', \omega))|\Delta z}, \frac{\omega^2}{v^2(x', k_x)} - k_x^2 < 0 \end{matrix} \right\}, k_z(k_x, x', \omega) = \sqrt{\frac{\omega^2}{v^2(x', k_x)} - k_x^2} \tag{4}$$

A major strength of this approach, compared to time domain Kirchoff methods for example, is that we need only consider the phase velocities. The group velocities, which are required for raytracing, are not needed because we treat each spectral component explicitly.

TRANSVERSE ISOTROPY

The angle dependant velocities of a TI media can be completely described by five elastic constants whose mathematical forms are well established. However, these constants are difficult to interpret physically. As a remedy, Thomsen (1986) derives the five elastic constants such that two of them are the physically realizable values of P-wave velocity (α_o) and S-wave velocity (β_o), measured at zero offset, plus three additional constants. Due to this simplicity we adopt the Thomsen derivations as input parameters for wavefield extrapolation.

In this paper we concentrate on the extrapolation of P-waves. It is our intention to provide an S-wave solution in the near future. By concentrating on P-waves the required number of parameters reduces to four. The P-wave velocity as a function of angle of incidence θ is:

$$v_p(\theta) = \alpha_o^2 \left[1 + \varepsilon \sin^2\theta + D^*(\theta)\right] \tag{5}$$

with

$$D^*(\theta) = \frac{1}{2}\left(1 - \frac{\beta_o^2}{\alpha_o^2}\right)\left\{\left[1 + \frac{4\delta^*}{\left(1-\beta_o^2/\alpha_o^2\right)}\sin^2\theta\cos^2\theta + \frac{4\left(1-\beta_o^2/\alpha_o^2+\varepsilon\right)\varepsilon}{\left(1-\beta_o^2/\alpha_o^2\right)^2}\sin^4\theta\right]^{\frac{1}{2}} - 1\right\} \tag{6}$$

We remind the reader that in the above TI equations each of the anisotropic parameters is a function of input position x'. For simplicity we have suppressed the x' dependence.

TI NSPS

Wavefield extrapolation by NSPS is an operation that loops over frequency; one monochromatic wavefield is extrapolated per loop. For efficiency we want to compute required TI calculations in such a way that as much computation as possible is done outside of the loop. Following Kitchenside (1991), we compute a set of horizontal slownesses (p) for a range of evenly spaced angles (θ). (For a non-zero symmetry axis we simply relate the angle of incidence of waves to the rotated axis of anisotropy). The set of *p* values are used to find a set of vertical slownesses (q) for a range of evenly spaced wavenumbers (k_x). The slowness values are computed using:

$$p(x',\theta) = \frac{\sin(\theta)}{v(x',\theta)} \tag{7}$$

$$q(x',\theta) = \frac{\cos(\theta)}{v(x',\theta)} \tag{8}$$

where $v(x',\theta)$ is computed using equations (5) and (6). Because *p* and *q* are independent of temporal frequency (ω) they both are computed outside of the main recursion. Then, for each ω, a new set of *p* values are computed using:

$$p(k_x,\omega) = \frac{k_x}{\omega} \tag{9}$$

which are then compared to $p(x',\theta)$ from equation (7). For the non-evanescent region a set of θ values are produced from this comparison and are used to compute a set of *q* values by equation (8), thereby relating k_x to θ. In the evanescent region the *q* values are computed using:

$$q(k_x,x',\omega) = -ip(x',\theta)_{\max}\sqrt{k_x^2 - w^2 p^2(x',\theta)_{\max}} \tag{10}$$

where we use the maximum horizontal slowness $\left(p(x',\theta)_{\max}\right)$ of the media to damp evanescent energy. The resulting set of q values are then used to calculate the values of the vertical wavenumbers $k_x = \omega q$ required for extrapolation:

$$\alpha(k_x, x', \omega) = e^{i\omega q(k_x, x', \omega)\Delta z}. \tag{11}$$

It is useful to combine equations (8), (10) and (11) into a single statement for comparison with equation (4):

$$\alpha(k_x, x', \omega) = e^{i\omega q(k_x, x')\Delta z}, \begin{cases} q(k_x, x') = Interp\left(q(x',\theta), p(x',\theta), \frac{k_x}{\omega}\right) \frac{k_x}{\omega} \le p(x',\theta)_{\max} \\ q(k_x, x') = -ip(x',\theta)_{\max}\sqrt{k_x^2 - \omega^2 p^2(x',\theta)_{\max}}, \\ \frac{k_x}{\omega} > p(x',\theta)_{\max} \end{cases} \tag{13}$$

Equation (13) shows that, in the non-evanescent region, $\alpha(k_x, x', \omega)$ is computed with the *interp* function. This function represents the interpolation scheme that finds $q(k_x, x')$ from $q(x',\theta)$ using $p(x',\theta)$ as an intermediary. In the evanescent region, $q(k_x, x')$ is computed using the familiar square root equation parameterized with the maximum value of p (the isotropic velocity).

EXAMPLES

To demonstrate TI NSPS we present a set of impulse responses for a number of different geologic settings. Each setting has unique anisotropic parameters and angle of symmetry. The resulting impulse responses are compared to those of the material with a vertical axis of TI symmetry, and the case of isotropy. From these comparisons we find some notable differences. These differences which are discussed in the context of vertical slowness.

Weathered gypsum

The anisotropic parameters for weathered gypsum are in Thomsen (1986) notation:

$$\alpha_o = 1991, \beta_o = 795, \varepsilon = 1.161, \delta^* = -1.075$$

If we think of the anisotropy of a material as the percent difference between the fast and slow directions we find that weathered gypsum has a maximum anisotropy of 80% at +/-90 incidence (Figure 1). Figures (2) through (4) show 3D plots of respectively, the velocity (Vp), horizontal slowness (p) and vertical slowness (q) of the material as a function of angle of incidence (θ) and angle of TI symmetry (φ). We can see that the p and q surfaces are relatively simpler than the velocity surface.

This is more clearly indicated by Figure (5) which is a plot of *q* anisotropy, achieving a maximum of 20% at +/- 52 degrees.

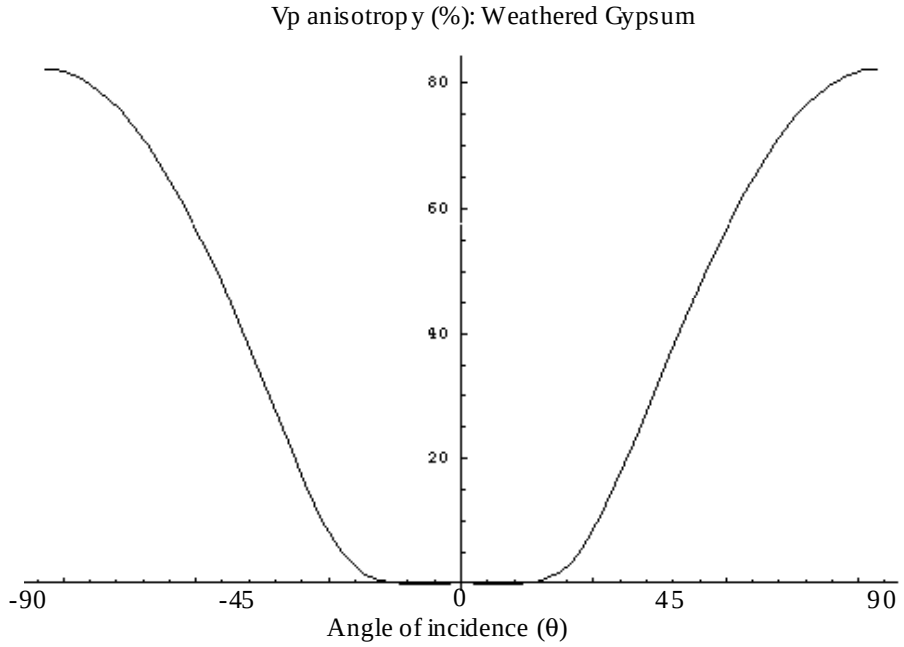

Fig. 1. P-wave anisotropy for weathered gypsum. The maximum anisotropy is 82% at +/- 90 degrees (assuming vertical TI symmetry).

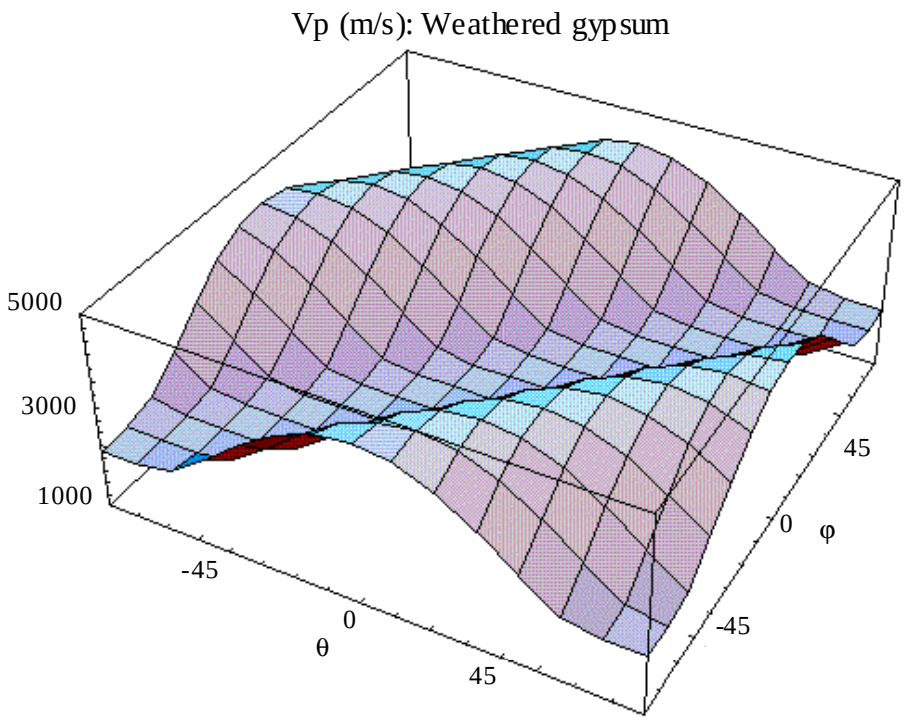

Fig. 2. P-wave velocity as a function of angle of incidence (θ) and TI symmetry axis (φ) for weathered gypsum.

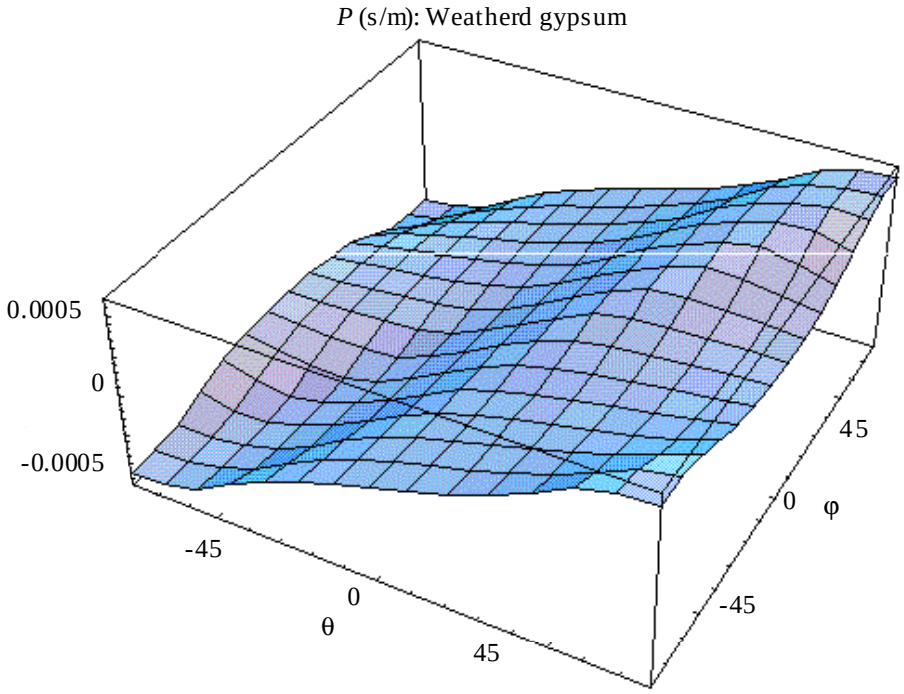

Fig. 3. Horizontal slowness (p) as a function of angle of incidence (θ) and TI symmetry axis (φ) for weathered gypsum.

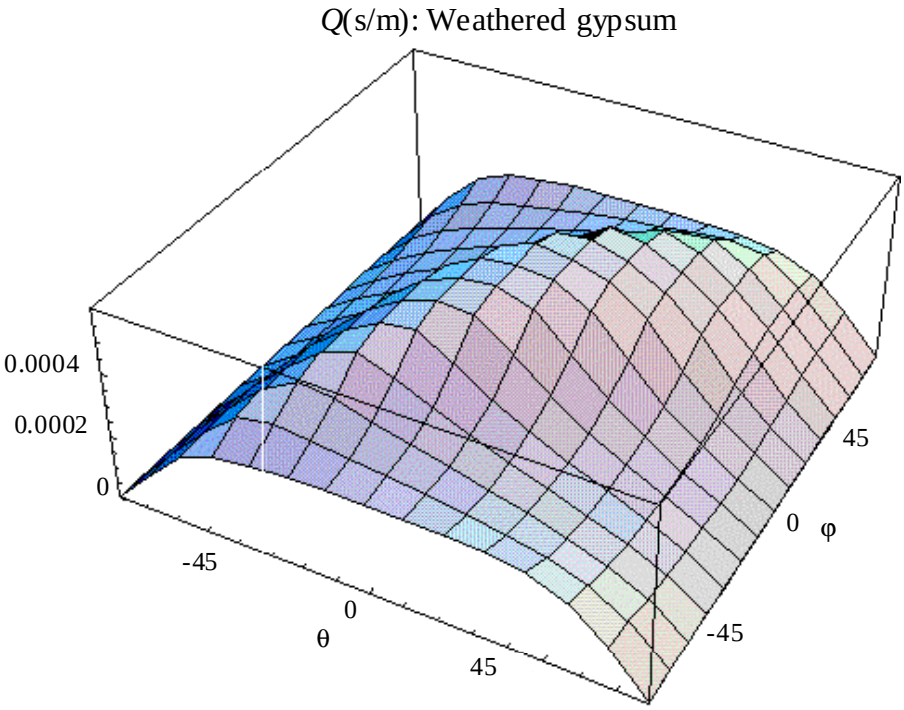

Fig. 4. Vertical slowness (q) as a function of angle of incidence (θ) and TI symmetry axis (φ) for weathered gypsum.

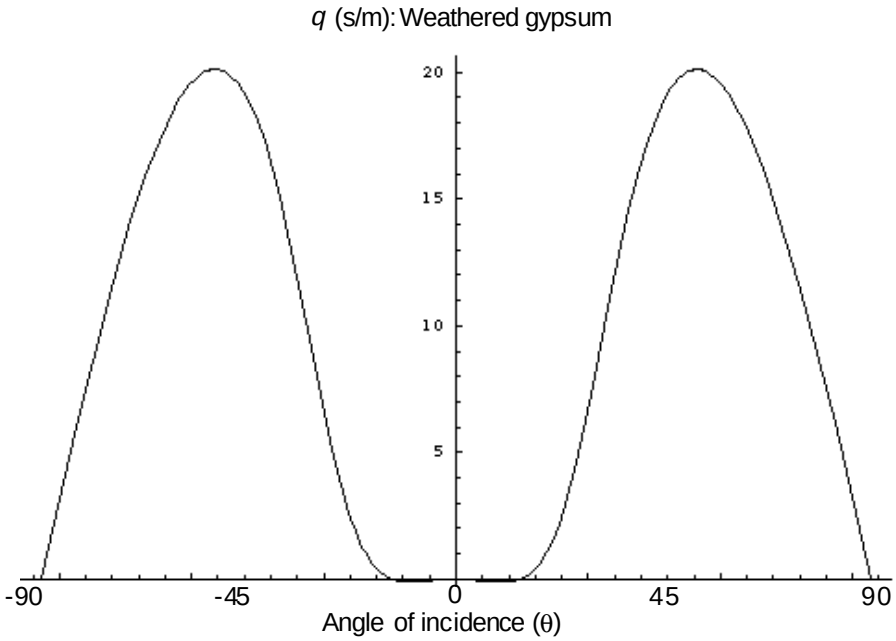

Fig. 5. q anisotropy for weathered gypsum. The maximum anisotropy is 20% at +/- 52 degrees (assuming vertical TI symmetry).

Impulse responses are generated by extrapolating a single spike through 300 m using a velocity model parameterized with no anisotropy $(\varepsilon = 0, \delta^* = 0)$, vertical TI, and TI with a -45 degree symmetry axis.

Discussion

The isotropic impulse response of Figure (6) is an upside down hyperbola showing numerical attenuation at the larger travel times. (This purpose of this effect is to suppress Fourier wraparound, and is achieved by adding a small imaginary component, calculated as a percentage, to the velocities). Comparison of this curve to the vertical TI impulse response of Figure (7) shows how the TI extrapolation is faster for higher dip angles and shows less numerical attenuation.

Figure (9) is a plot of q for the isotropic, vertical TI and TI with φ = -45 degrees, and is useful for understanding the impulse responses. We see that, due to anisotropy, the vertical TI extrapolation is computed with lower q than the isotropic example. Lower q means higher velocity and therefore shorter travel times through the same depth step. Shorter travel times can be seen in the impulse response as limbs which have less dip. The reduction in dip implies increased wavelength in the x direction and therefore reduced numerical attenuation effects thus, the vertical TI impulse response is less dispersed.

The impulse response for φ = -45 degrees is shown in Figure (8). We see that, compared to the isotropic curve, the TI response is skewed down and to the left. This

can be understood, again, with the help of Figure (9). The *q* curve for this non-vertical example is also skewed showing greater slowness for negative angles of incidence. If we think of a diffraction curve for this situation we see that waves incident along negatively dipping ray paths travel slower than those along positive ray paths thereby taking longer to traverse the same amount of depth. This changes as we follow the *q* curve from -90 degrees towards zero degrees where at about -20 degrees the trend reverses.

The diffraction curve for this example might be like the one pictured in Figure (10). If we then consider extrapolation as the cross correlation of the impulse with its diffraction response then a picture of the expected impulse response of the TI extrapolation emerges. It will look like a time and space reversed version of the diffraction response, and this is exactly what we see in Figure (8).

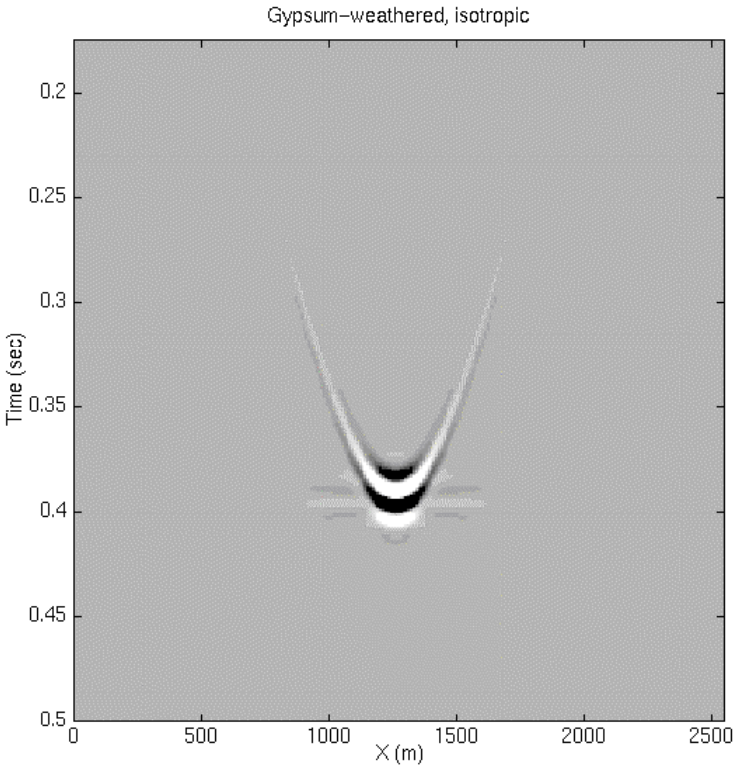

Fig 6. Isotropic impulse response for weathered gypsum.

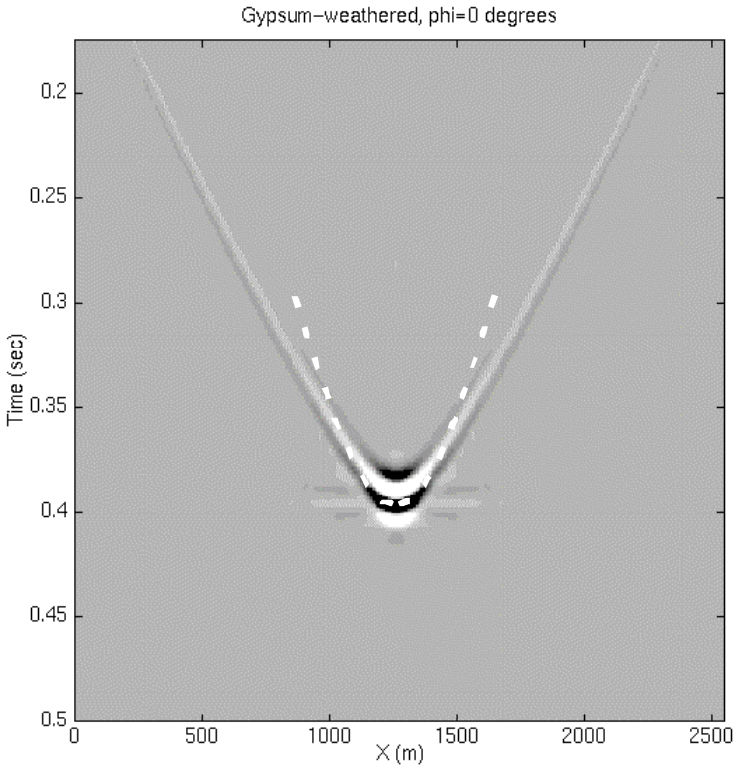

Fig. 7. Vertical TI impulse response for weathered gypsum. The isotropic response is overplotted in white.

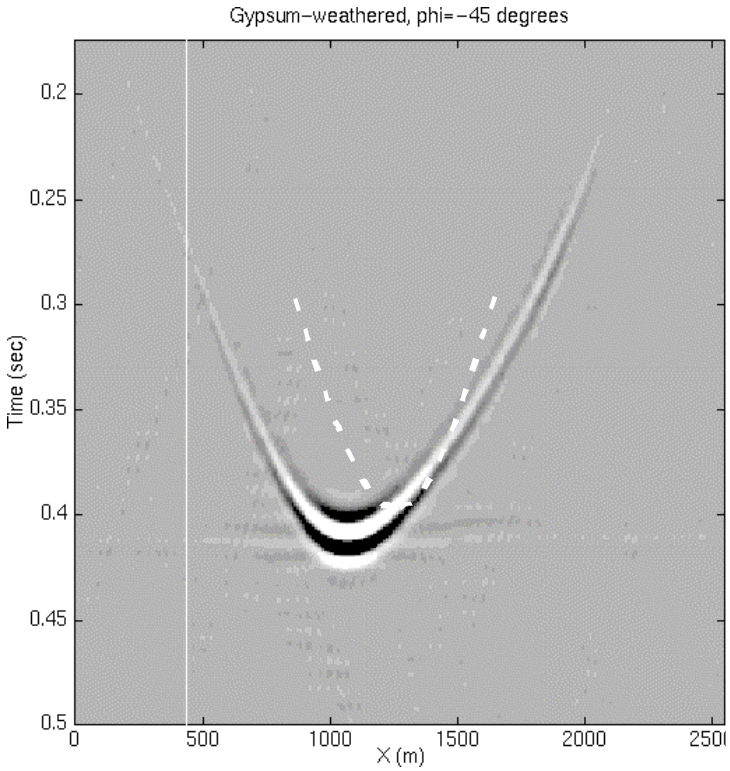

Fig. 8. TI impulse response for weathered gypsum. The isotropic response is overplotted in white.

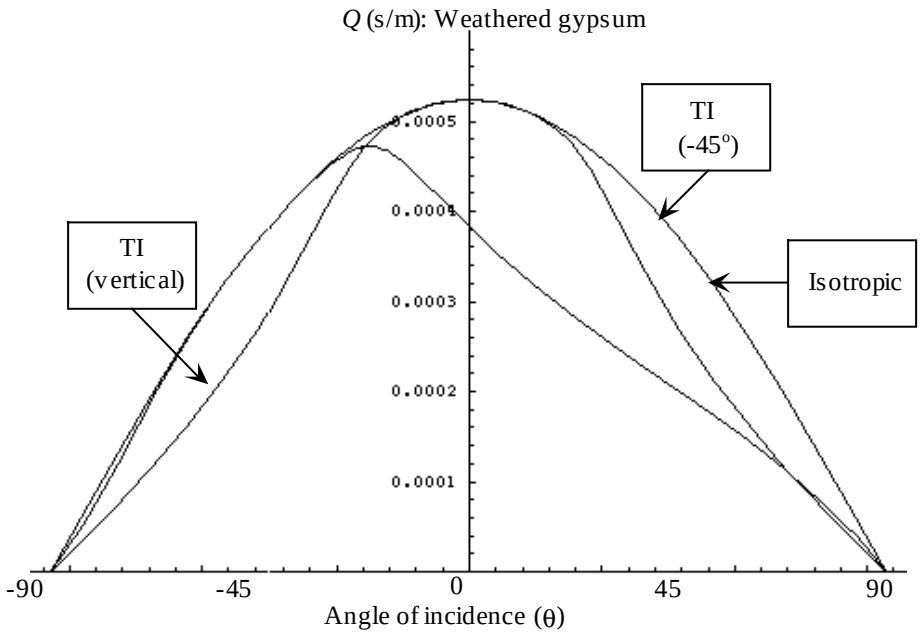

Fig. 9. Comparison of q, for different values of φ, as a function of θ . This plot is useful in understanding the skewed impulse response extrapolation through this medium (Figures 6, 7 and 8).

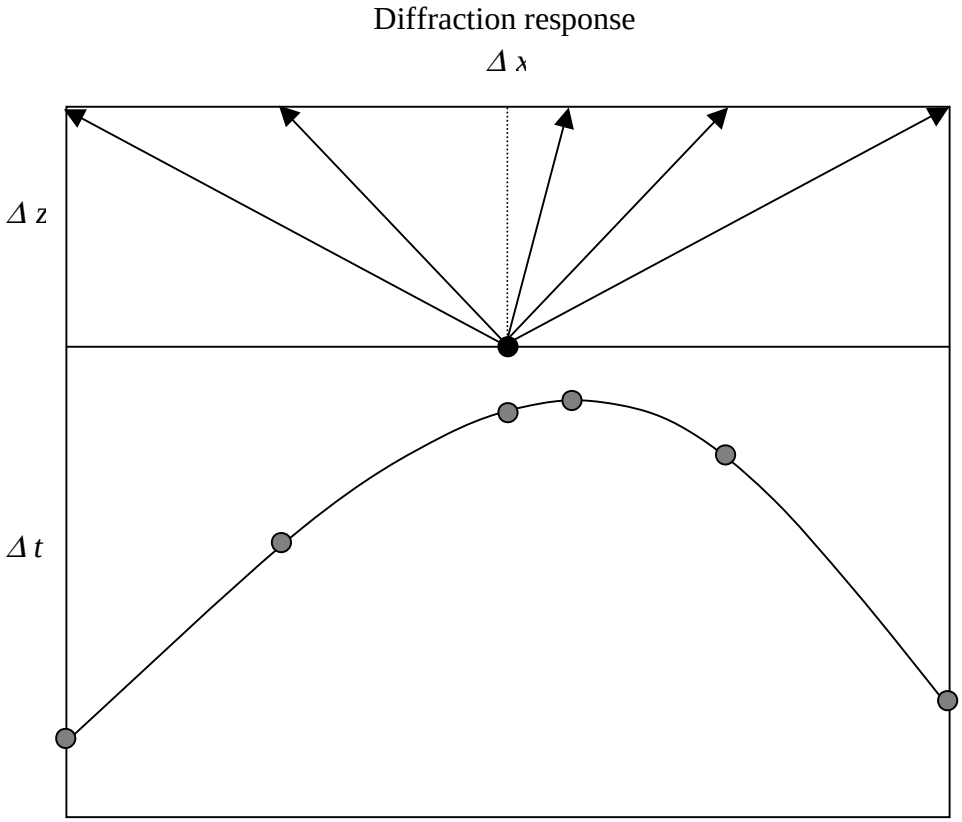

Fig. 10. TI diffraction response of a single impulse. The diffraction medium is weathered gypsum with a TI axis of symmetry of -45 degrees. The extrapolation impulse response is the time and space reversal of this curve (see Figure (9)).

Mesaverde shale

The second example is of a much more isotropic material: Mesaverde shale. The anisotropic parameters for this material are:

$$\alpha_o = 3901, \beta_o = 2682, \varepsilon = 0.137, \delta^* = -0.078$$

The maximum anisotropy of this material is about 13% at +/-90 incidence. Figure (11) shows a plot of P-wave anisotropy. Figures (12) through (14) show 3D plots of the P-wave velocity, *p* and *q* of this material as a function of θ and φ. Again we see that the *p* and *q* surfaces are relatively simple compared to the velocity surface, and much simpler than those for weathered gypsum. Figure (15) is a plot of *q* anisotropy, which achieves a maximum of 3.2% at +/- 60 degrees.

Again, impulse responses are generated by extrapolating a single spike through 300 m of the material using first an isotropic velocity model $(\varepsilon = 0, \delta^* = 0)$, then with vertical TI, and then a 60 degree symmetry axis.

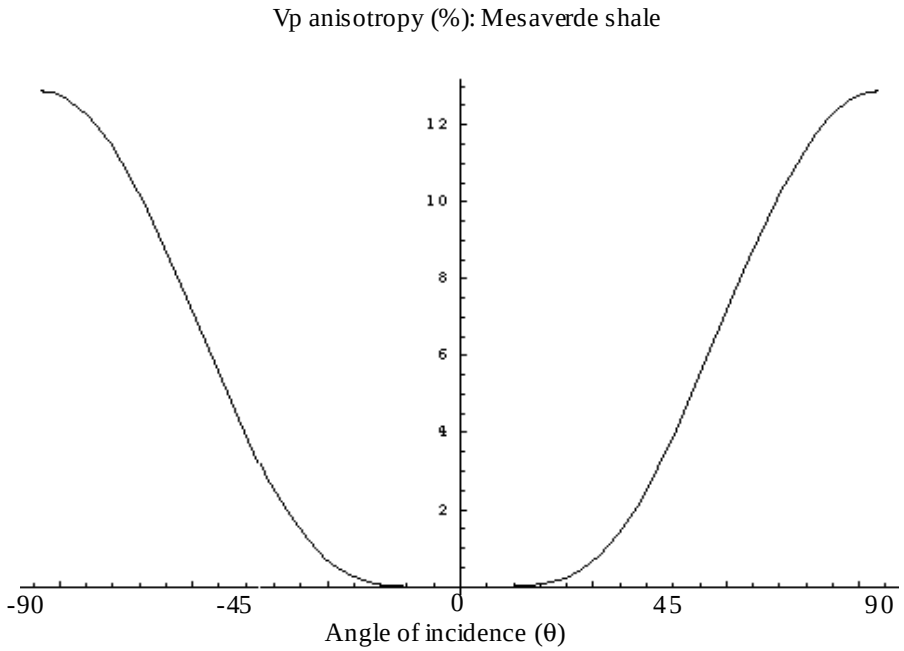

Fig. 11. P-wave anisotropy for Mesaverde shale. The maximum anisotropy is 13% at +/- 90 degrees (assuming vertical TI symmetry).

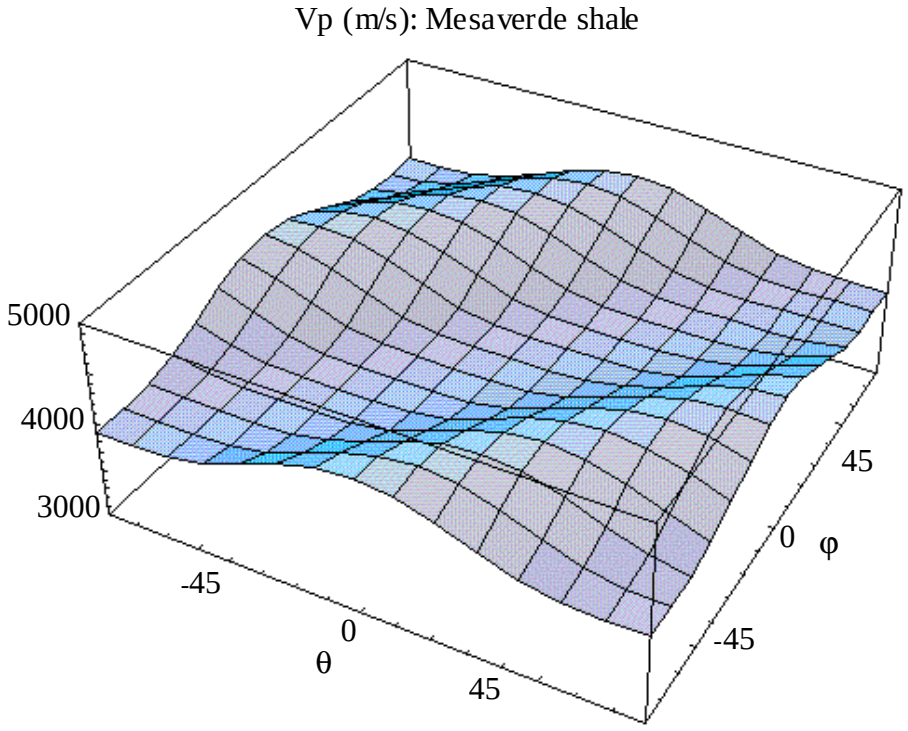

Fig. 12. P-wave velocity as a function of angle of incidence (θ) and TI symmetry axis (φ) for Mesaverde shale.

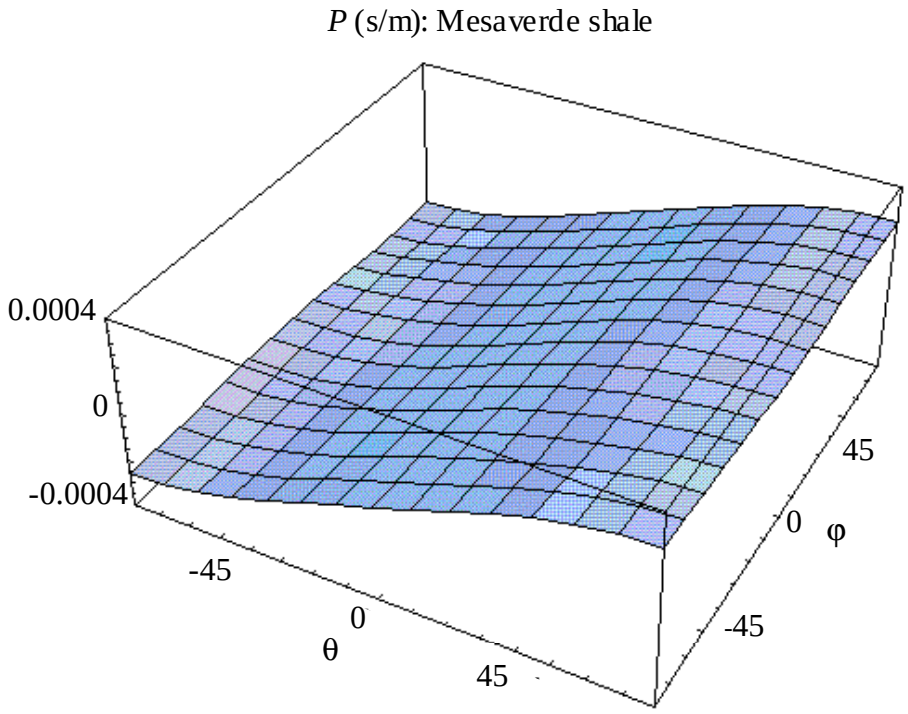

Fig. 13. Horizontal slowness (p) as a function of angle of incidence (θ) and TI symmetry axis (φ) for Mesaverde shale.

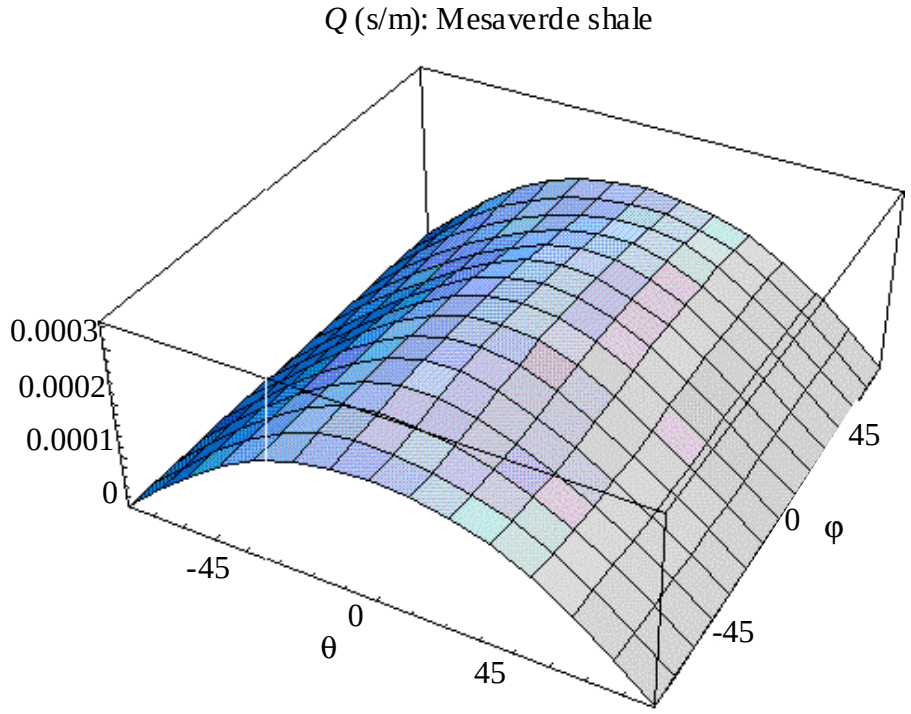

Fig. 14. Vertical slowness (q) as a function of angle of incidence (θ) and TI symmetry axis (φ) for Mesaverde shale.

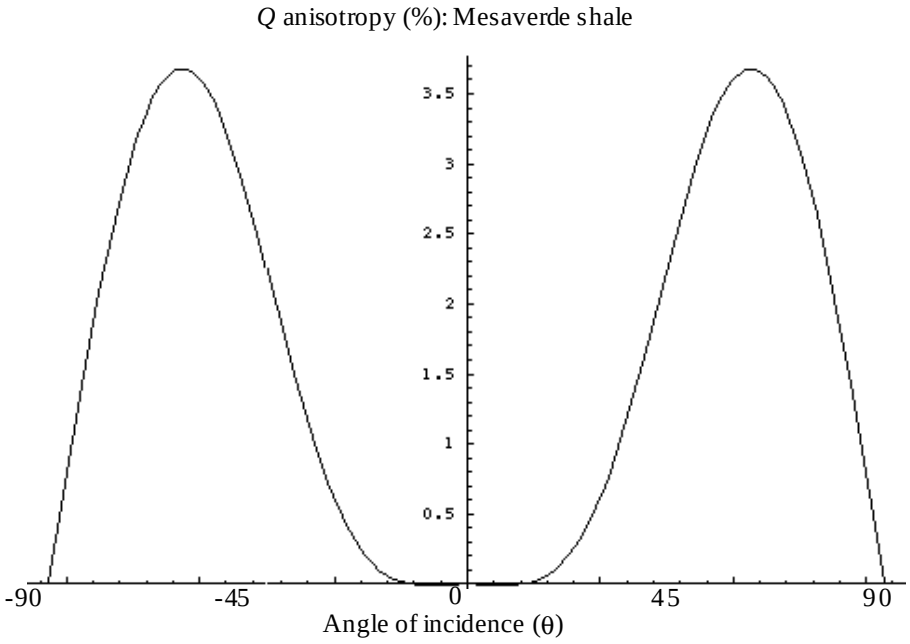

Fig. 15. *q* anisotropy for Mesaverde shale. The maximum anisotropy is 3.2% at +/- 60 degrees (assuming vertical TI symmetry).

Discussion

The isotropic, vertical TI and TI (φ = 60 degrees) impulse responses are given in Figures (16) to (18), and the corresponding q plot is shown in Figure (19). Comparison of Figures (16) and (17) shows that the vertical TI extrapolation is occurring faster for the higher angles of incidence, as in the gypsum example. From our previous discussion regarding the skew of the TI impulse response and its relation axis of symmetry and q (Figure 19) we expect it to be skewed down and to the right. The expected response is evident in Figure (18) though the effect is subtle compared to gypsum.

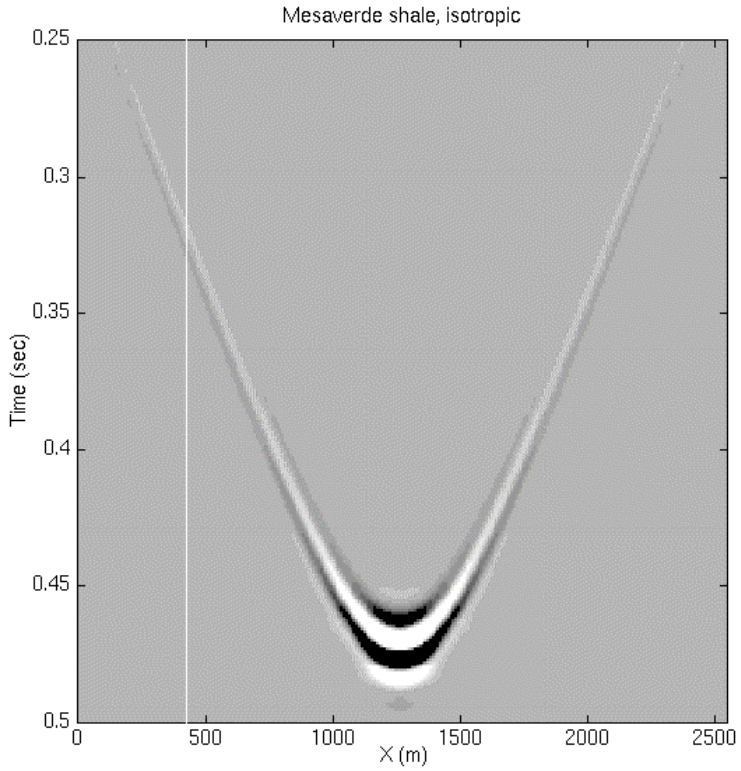

Fig 16. Isotropic impulse response for Mesaverde shale.

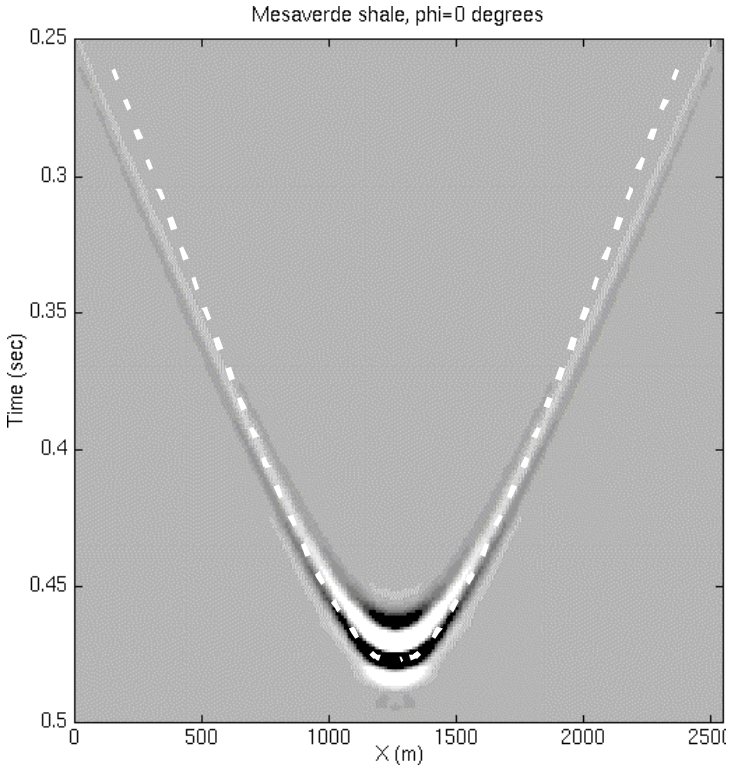

Fig. 17. Vertical TI impulse response for Mesaverde shale.The isotropic response is overplotted in white.

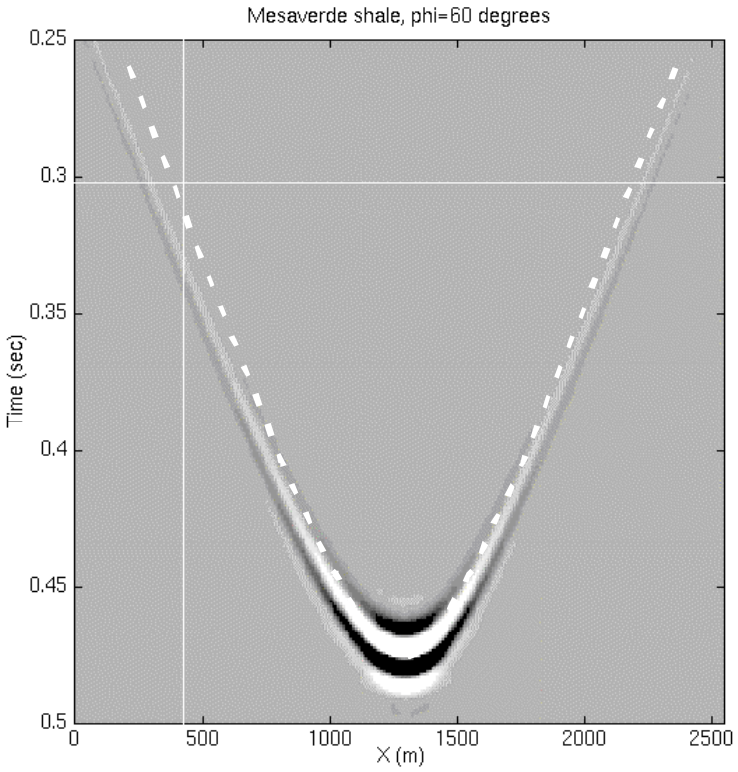

Fig. 18. TI impulse response for Mesaverde shale. The isotropic response is overplotted in white.

Weathered gypsum/Mesaverde shale

The final example is of a material that is a combination of the above to TI media. Figure (20) describes the geometry of this model in which 300m of Mesaverde shale meets abruptly with 300m of weathered gypsum. The anisotropyies of the two media are parameterized exactly as in the above two examples including the axes of symmetry.

For this TI model we extrapolate two spatially separate impulses simultaneously through the medium described in Figure (20). As indicated, the impulses are positioned such that, during translation through the medium, the one on the left encounters dipping weathered gypsum and the other encounters dipping Mesaverde shale.

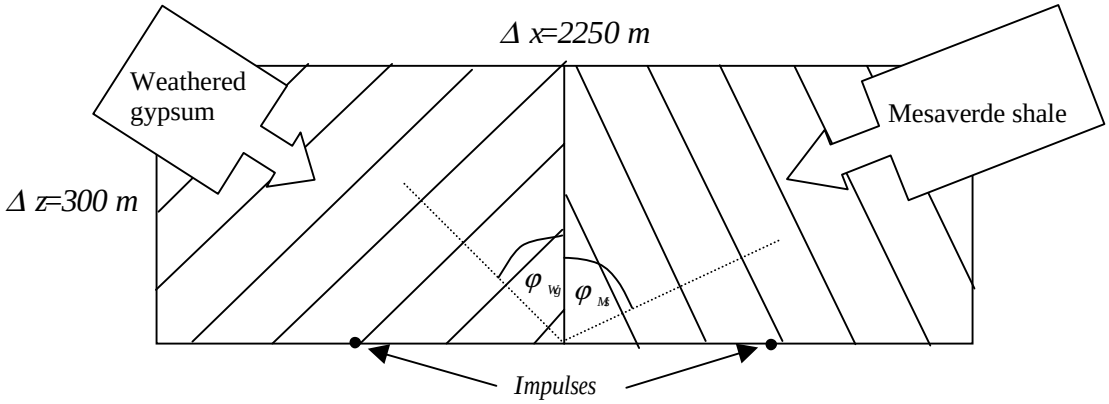

Fig. 20. Model of weathered gypsum and Mesaverde shale, $\varphi_{Wg} = -45$ degrees, $\varphi_{Ms} = 60$ degrees.

Discussion

As Figure (21) shows, we have achieved an extrapolated wavefield trough a media which is anisotropic and whose parameters vary with spatial position. The apparent boundary reflections are Fourier wraparound.

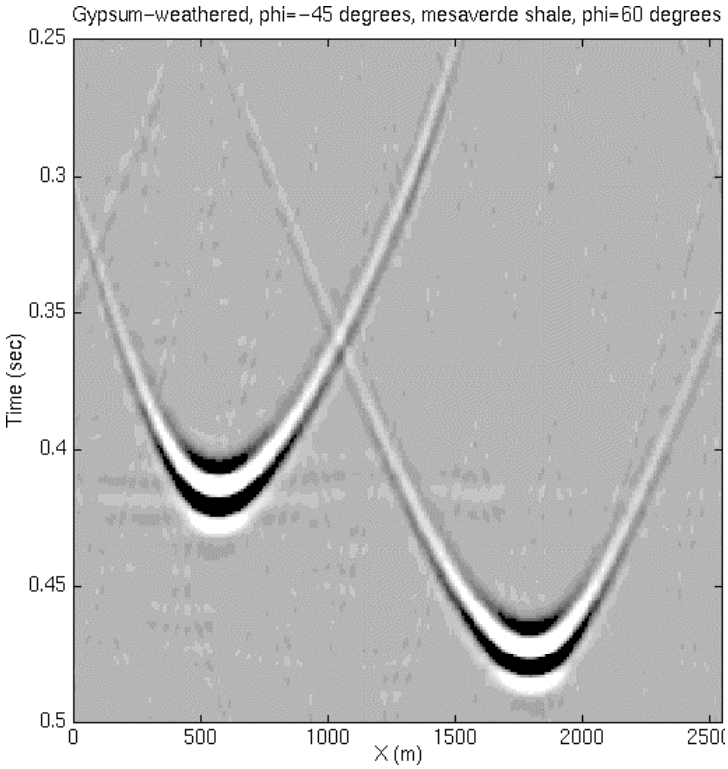

Fig. 21. TI impulse response for weathered gypsum/Mesaverde shale. A model of this material is given in Figure (20).

Conclusions

The theory of nonstationary filters, as applied to wavefield extrapolation, can describe extrapolation operators that vary laterally. The extension of this extrapolator to embrace variation with angle of incidence is presented in the context of transverse P-wave isotropy (TI). We show how standard nonstationary phase shift (NSPS) is modified, using vertical and horizontal slowness, to handle TI media with no restriction on the angle of TI symmetry. Thompson parameters are used to describe the anisotropy of the media. An advantage of our approach is that migration or modeling by TI NSPS requires knowledge of phase velocity alone.

We give P-wave impulse responses for NSPS extrapolation through different models of TI media. The first impulse response is for 300 meters of weathered Gypsum having a TI symmetry axis of –45 degrees. The second is for extrapolation through 300 meters of Mesaverde shale having an axis of 60 degrees. These two impulse responses are compared to their isotropic and zero degree counterparts. The Gypsum impulse response is found to show significant variation in shape, where the Mesaverde shale example is less so. These results are in agreement with analysis of velocities and horizontal slownesses which show Gypsum to have maximum anisotropy's respectively of 82% and 20% compared to 13% and 3% for Mesaverde shale.

We then present an example where two spatially separate impulses are extrapolated simultaneously through a 300-meter thick model consisting of Gypsum and Mesaverde shale with symmetry axes as described above. The two media are arranged in such a way that Gypsum grades abruptly into Mesaverde shale. This last example demonstrates the ability of NSPS to cope with lateral velocity variation simultaneously with angle of incidence.

References

Black, J. L., Su, C. B., Wason, C. B., 1984, Steep-D-p depth migration: Expanded abstracts, **54**th Annual Mtg. Soc. Expl. Geophy., 456-457.

Byun, B. B., 1984, Seismic parameters for transversely isotropic media: Geophysics, **49**, 1908-1914.

Crampin, S., 1984, Anisotropy in exploration seismics: First Break, 19-21.

Ferguson, R. J., and Margrave, G. F., 1997, Comparison of algorithms for nonstationary phase shift: CREWES Research Report, Vol. **9**, 31-1 - 31-19.

Isaac, J. H. and Lawton, D. C., 1997, Anisotropi physical modeling: Foothills Research Report, Vol. **3**, 15-1 - 15-26.

Kitchenside, P. W., 1991, Phase shift-based migration for transverse isotropy: **67**st Mtg., Soc. Expl. Geophys., Expanded Abstracts, 993-996.

Margrave, G. F., 1997, Theopry of nonstationary linear filtering in the Fourier domain with application to time variant filtering: Geophysics, *in press*.

Margrave, G. F., and Ferguson R. J., 1997, Wavefield extrapolation by nonstationary phase shift: Margrave, G. F., and Ferguson, R. J., 1997, Wavefield extrapolation by nonstationary phase shift: : Expanded abstracts, **67**th Annual Mtg. Soc. Expl. Geophy., 1599-1602.

Postma, G. W., 1955, Wave propagation in a stratified medium: Geophysics, **20**, 780-807.

Thomsen, L., 1986, Weak elastic anisotropy: Geophysics, **51**, 1954-1966.

Uzcategui, O., 1995, 2-D depth migration in transversely isotropic media using explicit operators: Geophysics, **60**, 1819-1829.

Wapenaar, C. P. A., 1992, Wave equation based seismic processing: In which domain?: EAGE **54**th Conference Extended Abstracts, B019.